microRNA-16-5p suppresses cell proliferation and angiogenesis in colorectal cancer by negatively regulating forkhead box K1 to block the PI3K/Akt/mTOR pathway

Xin Huang,[1]* Xuan Xu,[1]* Huajing Ke,[1] Xiaolin Pan,[1] Jiaoyu Ai,[1] Ruyi Xie[2] Guilian Lan,[1] Yang Hu,[1] Yao Wu[1]

[1]Department of Gastroenterology, The First Affiliated Hospital of Nanchang University, Jiangxi Clinical Research Center for Gastroenterology, Nanchang, Jiangxi

[2]Department of Gastroenterology, The Second Affiliated Hospital of Nanchang University, Jiangxi Clinical Research Center for Gastroenterology, Nanchang, Jiangxi, China

**These authors contributed equally to this research.*

ABSTRACT

MicroRNAs (miRNAs/miRs) have aroused increasing attention in colorectal cancer (CRC) therapy. This study is designed for a detailed analysis of the roles of miR-16-5p and forkhead box K1 (FOXK1) in cell angiogenesis and proliferation during CRC in addition to their underlying mechanisms. CRC tissues and colon cancer cell lines (SW620 and HCT8) were investigated. qRT-PCR and Western blot were utilized to evaluate miR-16-5p and FOXK1 expression. Following gain- and loss-of-function assays on miR-16-5p or FOXK1, the effects of miR-16-5p and FOXK1 were assessed on cell angiogenesis and proliferation in CRC cells. A dual-luciferase reporter assay was employed to evaluate the binding relationship of miR-16-5p and FOXK1. Western blot was used to determine the effects of miR-16-5p and FOXK1 on key molecules of the PI3K/Akt/mTOR pathway. Highly expressed FOXK1 and lowly expressed miR-16-5p were observed in CRC cells and tissues. miR-16-5p overexpression or FOXK1 knockdown reduced CRC cell proliferation and angiogenesis of human umbilical vein endothelial cells co-cultured with the supernatant of CRC cells, whereas miR-16-5p silencing or FOXK1 upregulation caused opposite trends. Additionally, miR-16-5p negatively modulated FOXK1 expression. The blockade of the PI3K/Akt/mTOR pathway was triggered by miR-16-5p overexpression or FOXK1 silencing. In conclusion, miR-16-5p hampers cell angiogenesis and proliferation during CRC by targeting FOXK1 to block the PI3K/Akt/mTOR pathway.

Key words: microRNA-16-5p; forkhead box K1; PI3K/Akt/mTOR pathway; colorectal cancer; proliferation; angiogenesis.

Correspondence: Yao Wu, Department of Gastroenterology, The First Affiliated Hospital of Nanchang University, Jiangxi Clinical Research Center for Gastroenterology, No.17 Yongwaizheng Road, Donghu District, Nanchang, Jiangxi 330008, China.
Tel. +86.15079086226. E-mail: wuyaodmn@126.com

Conflict of interest: The authors declare there is no conflict of interests.

Funding: Thanks for the grants from the Youth Science Project of Jiangxi Provincial Department of Science and Technology (No. 20181BAB215024) and the Youth Science Foundation of Jiangxi Provincial Department of Education (No. GJJ160242).

Contributions: HX, XX, contributed equally to the manuscript, had full access to all of the data in the study and take responsibility for the integrity of the data, the accuracy of the data analysis; WY, PXL, wrote the manuscript draft; AJY, performed research; XRY, KHJ, contributed substantially to the study design and the writing of the manuscript; LGL, HY, contributed to the manuscript preparation and statistical analysis. All the authors have read and approved the final version of the manuscript and agreed to be accountable for all aspects of the work.

Ethics approval and consent to participate: The study protocol concerning human study was approved by the Ethics Committee of The First Affiliated Hospital of Nanchang University, and all the patients provided their written informed consents.

Availability of data and materials: The datasets used or analyzed during the current study are available from the corresponding author on reasonable request.

Introduction

Colorectal cancer (CRC), consisting of colon cancer and rectal cancer, is the third prevailing cancer and the fourth cause frequently associated with cancer-caused death globally, accounting for roughly 600,000 deaths and 1.2 million new cases per year.[1,2] CRC is a lethal carcinoma worldwide with complicated pathogenesis, in which both environmental variables and genetic factors assume certain roles.[3] The treatment for CRC in clinical practice comprises radiation therapy, surgical resection, chemotherapy, adjuvant treatment, and immunotherapy.[4] Although great advancements have been achieved for CRC remedy, the five-year survival rate of metastatic CRC remains less than 10%, posing a serious threat to human mental and physical health. Therefore, it is of great significance to identify and understand changes in the cancer genome for targeted therapeutics development. Since the requirement of new vessels to provide nutrients and oxygen to the blood, angiogenesis elicits a major effect on the formation and progression of solid tumors.[5] The presence of angiogenesis interferes with a series of events triggered by the upregulation in angiogenic factors, such as microvessel density and vascular endothelial growth factor (VEGF).[6] As a type of endogenous small non-coding RNAs, microRNAs (miRNAs or miRs) negatively mediate the expression of the target genes by binding to the 3'-untranslated region of target messenger RNA transcripts for degradation or translational suppression.[7] Several miRNAs are uniformly associated with cell proliferation, angiogenesis, and metastasis in CRC, indicating that miRNAs may serve as therapeutic targets or diagnostic markers for CRC.[8,9] Growing evidence expounds that certain changes in miRNAs that mediate the expression of anti-oncogenes or oncogenes may also stimulate the occurrence of CRC.[10] Numerous studies have confirmed that miR-16, as a tumor suppressor, is involved in various cancers, including pancreatic cancer, prostate cancer, ovarian cancer, and CRC.[11-14] Briefly, miR-16 can repress cell survival, proliferation, angiogenesis, and epithelial-to-mesenchymal transition in CRC by targeting oncogenes.[15] The miR-16-5p/ALDH1A3/PKM2 axis modulates aerobic glycolysis and thus participates in the inhibition of CRC development through the diethyldithiocarbamate-copper complex.[16] Therefore, the mechanism of miR-16-5p in CRC merits further exploration.

The forkhead box K (FOXK) family regulates a variety of biological processes, such as cell cycle progression, differentiation, metabolism, and apoptosis.[17] Importantly, FOXK1 plays a crucial role in the orchestration of cell proliferation and differentiation in cancers.[18] For instance, Wang *et al.*[19] have reported that FOXK1 is highly expressed in gastric cancer (GC) tissues, which was responsible for the malignant behaviors of GC. Furthermore, the alteration of FOXK1 was documented to govern hilar cholangiocarcinoma cell migration and proliferation.[20] In CRC, FOXK1 is well documented to act as an oncogene.[21,22] Despite the oncogenic role of FOXK1 in several tumors having been elucidated, further research is needed to dissect the relationship between FOXK1 and miR-16-5p and the impacts of this relationship on CRC cells. Here, we were devoted to determining the relationship between FOXK1 and miR-16-5p and the impact of miR-16-5p/FOXK1 axis on cell proliferation and angiogenesis in CRC, hoping to shed light on a new insight into the disease mechanism and treatment of CRC.

Materials and Methods

Subjects and sample collection

From June 2018 to December 2018, 20 pathologically diagnosed CRC patients were included in this study with their CRC tissues and adjacent tumor tissues (at least 2 cm away from tumor lesion) collected. After surgical resection of the tumor, samples were immediately collected, frozen in liquid nitrogen, and then stored at -80°C until being used. Through pathological diagnosis, tumor tissue specimens were clearly diagnosed as CRC, and adjacent tumor tissues were clearly excluded from CRC. The included CRC patients did not receive any anti-tumor therapy, such as neoadjuvant radiotherapy, chemotherapy, or traditional Chinese medicine before the surgery. No other concomitant malignant tumor was found in all eligible patients. The study protocol involving humans was approved by the Ethics Committee of The First Affiliated Hospital of Nanchang University, and all of the patients provided their written informed consents.

Cell culture

Human embryonic kidney cells (HEK293T), human umbilical vein endothelial cells (HUVECs), normal colorectal epithelial cells NCM460, and colon cancer cell lines (SW620 and HCT8) were obtained from Shanghai Institutes for Biological Science, Chinese Academy of Sciences (Shanghai, China). Cells were incubated with Dulbecco's modified eagle medium/nutrient mixture F-12 (Invitrogen, Carlsbad, CA, USA) encompassing 10% fetal bovine serum in a 37°C and 5% CO_2 incubator (ThermoFisher, Waltham, MA, USA). Cells were grown for 2-3 days before being harvested. Then, cells were passaged when cell confluence reached 70-90%, and cells in the logarithmic growth phase were harvested for follow-up experiments.

Quantitative real-time polymerase chain reaction (qRT-PCR)

Total RNA was extracted from CRC cells with TRIzol (Invitrogen). The cDNA template was synthesized using a reverse transcription kit (TaKaRa, Tokyo, Japan) based on the protocols. Gene expression was detected on a LightCycler 480 real-time polymerase chain reaction instrument (Roche Diagnostics, Indianapolis, IN, USA). The reaction conditions were concordant with the manuals of the fluorescent quantitative polymerase chain reaction kit (SYBR Green Mix, Roche Diagnostics). The thermal cycle parameters were 95°C for 10 s, followed by 45 cycles of 95°C for 5 s, 60°C for 10 s, and 72°C for 10 s, and a final extension at 72°C for 5 min. The test was implemented in triplicate. With U6 or glyceraldehyde-3-phosphate dehydrogenase (GAPDH) as the normalizer, data analysis was performed with the $2^{-\Delta\Delta Ct}$ method: $\Delta\Delta Ct = [Ct_{(target\ gene)}\text{-}Ct_{(reference\ gene)}]_{experimental\ group}\text{-}[Ct_{(target\ gene)}\text{-}Ct_{(reference\ gene)}]_{control\ group}$.

The primers are exhibited in Table 1.

Table 1. Primer sequences.

Name of primer	Sequences
miR-16-5p-F	GCTAGCAGCACGTAAATA
miR-16-5p-R	CGTGGAGTCGGCAAT
U6-F	CTCGCTTCGGCAGCACA
U6-R	AACGCTTCACGAATTTGCGT
FOXK1-F	AGCAGTGTACCTTCCGGTTTC
FOXK1-R	GTGGATCTTCAGAGGGGAGATC
GAPDH-F	GACAGTCAGCCGCATCTTCT
GAPDH-R	GCGCCCAATACGACCAAATC

F, forward; R, reverse.

Cell transfection and grouping

miR-16-5p mimic and its negative control (mimic NC) (100 nM), miR-16-5p inhibitor and inhibitor NC (100 nM), and pcDNA3.1-FOXK1 and its empty vector pcDNA3.1 (2 μg) were synthesized and constructed by GenePharma (Shanghai, China). Transfection was conducted with the Lipofectamine 2000 transfection kit (Invitrogen) as per the manuals. Following cell transfection, cells were assigned into a miR-16-5p mimic group, a mimic NC group, a miR-16-5p inhibitor group, an inhibitor NC group, a pcDNA3.1-FOXK1 group, a pcDNA3.1 group, a small interfering RNA (si)-FOXK1 group, and an si-NC group. Subsequent to 48-h transfection, the relative expression was tested.

Cell counting kit (CCK)-8 assay

Cells were seeded onto 96-well plates, made into 100 μl/well of cell suspension (1500 cells/well), and pre-cultured for 24 h in a 37°C and 5% CO_2 incubator. Then, each well of the plates was supplemented with 10 μL CCK-8 solution for further 2-h culture, and no bubble was created during this operation. Absorbance (optical density, OD) was measured at 450 nm with a microplate absorbance reader. The experiment was repeated three times. The absorbance value A was measured and the proliferation rate was reckoned: proliferation rate (%) = $[A_{(transfection\ group)} - A_{(Control)}]/[A_{(Blank\ group)} - A_{(Control)}] \times 100\%$. In the formula, $A_{(transfection\ group)}$ referred to the absorbance value of the wells encompassing cells subjected to cell transfection and culture with CCK-8 solution, $A_{(Control)}$ indicated the absorbance value of the wells containing culture medium and CCK-8 solution but without cells, and $A_{(Blank\ group)}$ represented the absorbance value of the wells encompassing cells without cell transfection but incubated with CCK-8 solution.

5-ethynyl-2'-deoxyuridine assay

Cell proliferation was determined utilizing 5-ethynyl-2'-deoxyuridine (EdU) assay following the protocols of an EdU assay kit (RiboBio, Guangzhou, China). Immunostaining was then observed under a Leica DMI3000B microscope with positive cells counted. The experiment was repeated three times.

Flow cytometry analysis

Cell suspension (1 ml) was seeded onto 6-well plates at the density of 5×10^5 cells/well, followed by incubation in an incubator at 37°C with 5% CO_2. After 24-h incubation, adherent cells were trypsinized and washed with pre-cooled phosphate-buffered saline twice (2,000 rpm, 5 min). After that, cells were re-suspended with 1 mL Annexin V binding buffer and then subjected to the 30-min reaction with 10 μL propidium iodide and 5 μL Annexin V-fluorescein isothiocyanate in the dark. Cell apoptosis was analyzed on a flow cytometer within 1 h. The experiment was repeated three times.

Tube formation assay

After trypsinization, cells were titrated into single-cell suspension before 5-min centrifugation at 12,000 rpm to obtain the supernatant. The supernatant was mixed with an equal volume of fresh medium to prepare a mixed solution for the culture of HUVECs. Before the tube formation assay, Matrigel, 24-well plates, and a pipette tip were liquefied/pre-cooled overnight at 4°C. HUVECs were exposed to a serum-free medium for 24-h serum-starved cell culture. Briefly, 250 μL chilled Matrigel solution was dispensed into the pre-chilled 24-well plates and allowed to solidify (37°C, 30 min), and no bubble was created during this operation. Following digestion with 0.25% Trypsin-Ethylenediaminetetraacetic Acid solution, HUVECs were titrated to single-cell suspension (7.5×10^6 cells/mL) using a 10% serum culture medium. After 10 μL single-cell suspension was mixed with 300 μL serum culture medium, the mixture was added to the pre-treated 24-well plates. Following 10-h conventional incubation, images were captured by microscopy, and the branch number and length of the formed tubes were measured and recorded. Data were obtained from three independent experiments.

Western blot

Cells were lysed with radio-immunoprecipitation assay lysis buffer (Beyotime, Shanghai, China) to obtain protein samples. After the protein concentration was measured by a bicinchoninic acid kit (Beyotime), the corresponding volume of protein was added and mixed with loading buffer (Beyotime) in a boiling-water bath for 3-min denaturation. Electrophoresis was conducted for 30 min at 80 V and then for 1-2 h at 120 V once bromphenol blue reached the separation gel. Then, the proteins were transferred to membranes at 100 V for 180 min in an ice bath. The membranes were rinsed 1-2 min with the washing solution and then blocked in the blocking solution at room temperature for 60 min or overnight at 4°C. The polyvinylidene fluoride membranes were incubated with the primary antibodies (1:1000) against GAPDH (5174S; Cell Signaling Technology, Beverly, MA, USA), FOXK1 (ab18196; Abcam, Cambridge, UK), phosphoinositide 3-kinase (PI3K, 17366S; Cell Signaling Technology), AKT (4685S; Cell Signaling Technology), and mechanistic target of rapamycin (mTOR, 2983S; Cell Signaling Technology), VEGFA (ab46154; Abcam), Angiopoietin 2 (ang2, ab153934; Abcam), matrix metalloproteinase-9 (MMP-9, ab76003; Abcam) at room temperature in a shaking table for 1 h. After that, the membranes were washed thrice with washing solution for 10 min and then incubated with goat anti-rabbit Immunoglobulin G (1:5000, Beijing ComWin Biotech Co., Ltd., Beijing, China) labeled with horseradish peroxidase for 1 h at room temperature. The membranes were washed with washing solution for 3×10 min prior to color development. Afterward, a chemiluminescence imaging analysis system (Bio-rad, Hercules, CA, USA) was applied for observation.

Dual-luciferase reporter assay

StarBase (http://starbase.sysu.edu.cn/) was utilized to predict the binding site of miR-16-5p to FOXK1. The mutant (mut) and wild-type (wt) sequences containing the binding sites of miR-16-5p to FOXK1 (mut-FOXK1 and wt-FOXK1) were designed and synthesized based on the predicted results and cloned into luciferase reporter vectors (pGL3-Basic). Thereafter, the designed sequences were co-transfected with miR-16-5p mimic (0, 150, 300 nM, GenePharma) into HEK293T cells, respectively. After that, cells received 20-min cell lysing with 100 μL cell lysis buffer on a shaking table at room temperature. Firefly luciferase activity or Renilla luciferase activity was measured after the exposure of cell suspension (50 μL) to luciferase reaction solution (50 μL, Promega, Madison, WI, USA) or Stop & Glo reagent (50 μL, Promega). The relative activity was calculated as the ratio of Firefly luciferase activity to Renilla luciferase activity. Renilla luciferase activity was regarded as an internal control. Three replicates were set for this test.

Statistical analysis

Statistical analysis was conducted utilizing GraphPad prism 7 software with the Shapiro-Wilk method for normality analysis and the Levene test for homoscedasticity analysis. The correlation between miR-16-5p and FOXK1 expression was analyzed with the Pearson correlation coefficient. The *t*-test was employed for the comparison between the two groups. Comparisons among multiple groups were analyzed with a one-way analysis of variance test, followed by Tukey's *post-hoc* test. Western blots were analyzed using Image J (version 1.6065; National Institutes of Health).

Experiments were repeated three times. Data were displayed as mean ± standard deviation (SD), and all sample data conformed to normal distribution and homoscedasticity; p-values of significance were $p<0.05$.

Results

CRC tissues and cells exhibited highly expressed FOXK1 and lowly expressed miR-16-5p

Here, miR-16-5p expression in CRC and tumor-adjacent tissues was measured with qRT-PCR (Figure 1A). CRC tissues had considerably lower miR-16-5p expression than tumor-adjacent tissues. As expected, qRT-PCR unfolded an increased FOXK1 mRNA level in CRC tissues (Figure 1A, *vs* tumor-adjacent tissues). Additionally, miR-16-5p was negatively correlated with FOXK1 as shown by the Pearson correlation coefficient (Figure 1B, $p<0.05$). Similar results were obtained from qRT-PCR and Western blot analyses on the colon cancer cell lines (SW620 and HCT8), which exhibited an increase of FOXK1 expression and a decrease of miR-16-5p expression in SW620 and HCT8 cells compared with normal colorectal epithelial cell NCM460 (Figure 1 C-F). These preliminary observations indicated a negative correlation between abnormally expressed miR-16-5p and FOXK1 in CRC.

miR-16-5p facilitated cell apoptosis and inhibited cell angiogenesis and proliferation in CRC

The effects of miR-16-5p on cell proliferation and angiogenesis were dissected. qRT-PCR revealed the satisfactory transfection of miR-16-5p mimic or miR-16-5p inhibitor in SW620 and HCT8 cells (Figure 2A; $p<0.05$). To measure CRC cell proliferation, CCK-8 and EdU assays were implemented. Notably, a pronounced elevation in proliferation was found in CRC cells transfected with miR-16-5p inhibitor (*vs* inhibitor NC, $p<0.05$), and a marked decline in CRC cell proliferation was shown after miR-16-5p mimic transfection (Figure 2 B,C; *vs* mimic NC, $p<0.05$). CCK-8 and EdU assay results presented the inhibitory influence of miR-16-5p on CRC cell proliferation.

As reflected by flow cytometry results, there were an elevated proportion of apoptotic cells in SW620 and HCT8 cells transfected with miR-16-5p mimic (Figure 2D; *vs* mimic NC, $p<0.05$) and reduced apoptotic rate in CRC cells treated with miR-16-5p inhibitor (Figure 2D; *vs.* inhibitor NC, $p<0.05$). These findings suggested that miR-16-5p accelerated CRC cell apoptosis.

Angiogenesis is indispensable for the progression and development of tumor cells. With respect to the tube-forming ability of HUVECs, HUVECs cultured in the supernatant of SW620 and HCT8 cells transfected with miR-16-5p mimic had reduced tube-forming ability and expression of angiogenesis-related proteins (VEGFA, ang2, and MMP-9), but HUVECs cultured in the super-

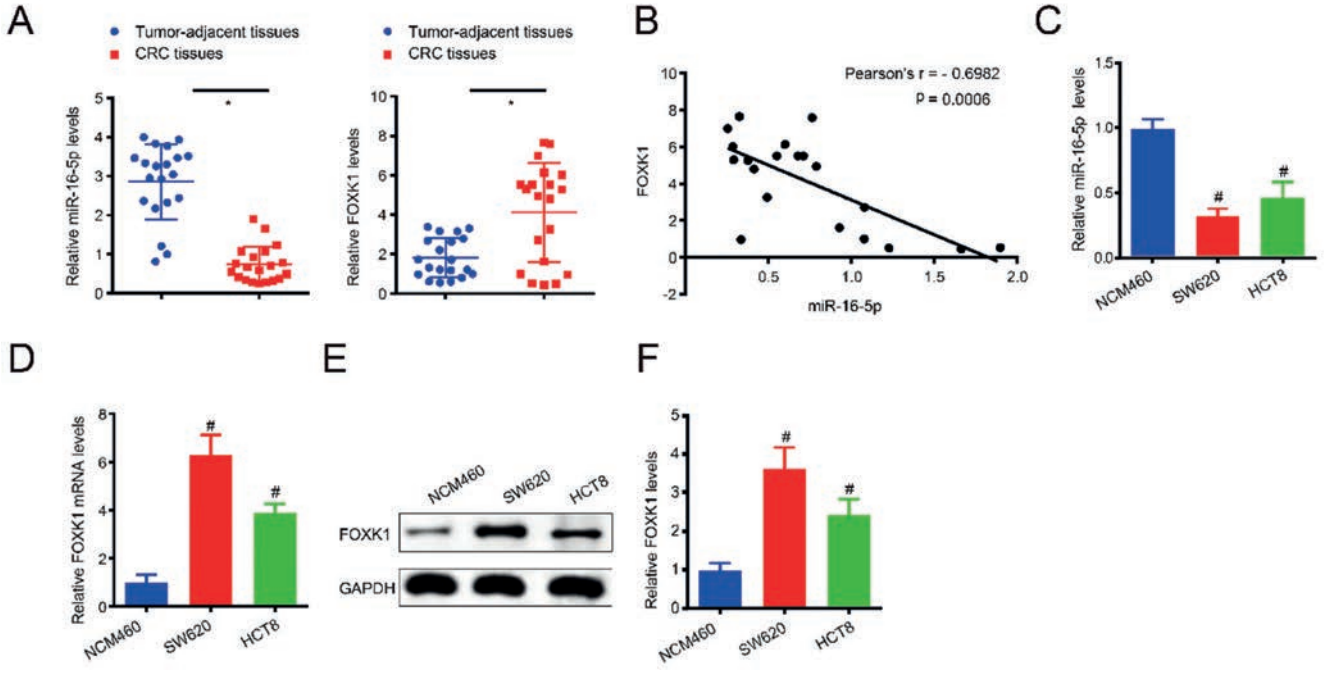

Figure 1. CRC cells have elevated level of FOXK1 and suppressed level of miR-16-5p. A) Lowly expressed miR-16-5p (left) and highly expressed FOXK1 (right) in CRC tissues were quantitated by qRT-PCR. B) Pearson correlation coefficient analysis identified the negative correlation of miR-16-5p with FOXK1. C) miR-16-5p expression in colon cancer cell lines (SW620 and HCT8) and normal colorectal epithelial cell NCM460 was measured by qRT-PCR. (D) FOXK1 mRNA expression in SW620, HCT8, and NCM460 cells was evaluated by qRT-PCR. E) Representative Western blots of FOXK1 protein in SW620, HCT8, and NCM460 cells were presented. F) FOXK1 protein expression in SW620, HCT8, and NCM460 cells was evaluated by Western blot; *t*-test was applied for comparison between two groups, and one-way analysis of variance test for comparison among multiple groups, with Tukey's method for *post-hoc* multiple comparisons. Cell experiments were independently repeated three times, and data were expressed as means ±SD. CRC, colorectal cancer; #p<0.05 compared to the NCM460 group; *p<0.05 compared to the tumor-adjacent tissues.

natant of SW620 and HCT8 cells transfected with miR-16-5p inhibitor had opposite trend (Figure 2 E,F; $p<0.05$). The observed findings illustrated that miR-16-5p upregulation restricted cell proliferation and angiogenesis in CRC.

FOXK1 promoted cell proliferation and angiogenesis and repressed cell apoptosis in CRC

Here, the role of FOXK1 in CRC cell proliferation was explored. Results of Western blot and qRT-PCR manifested the

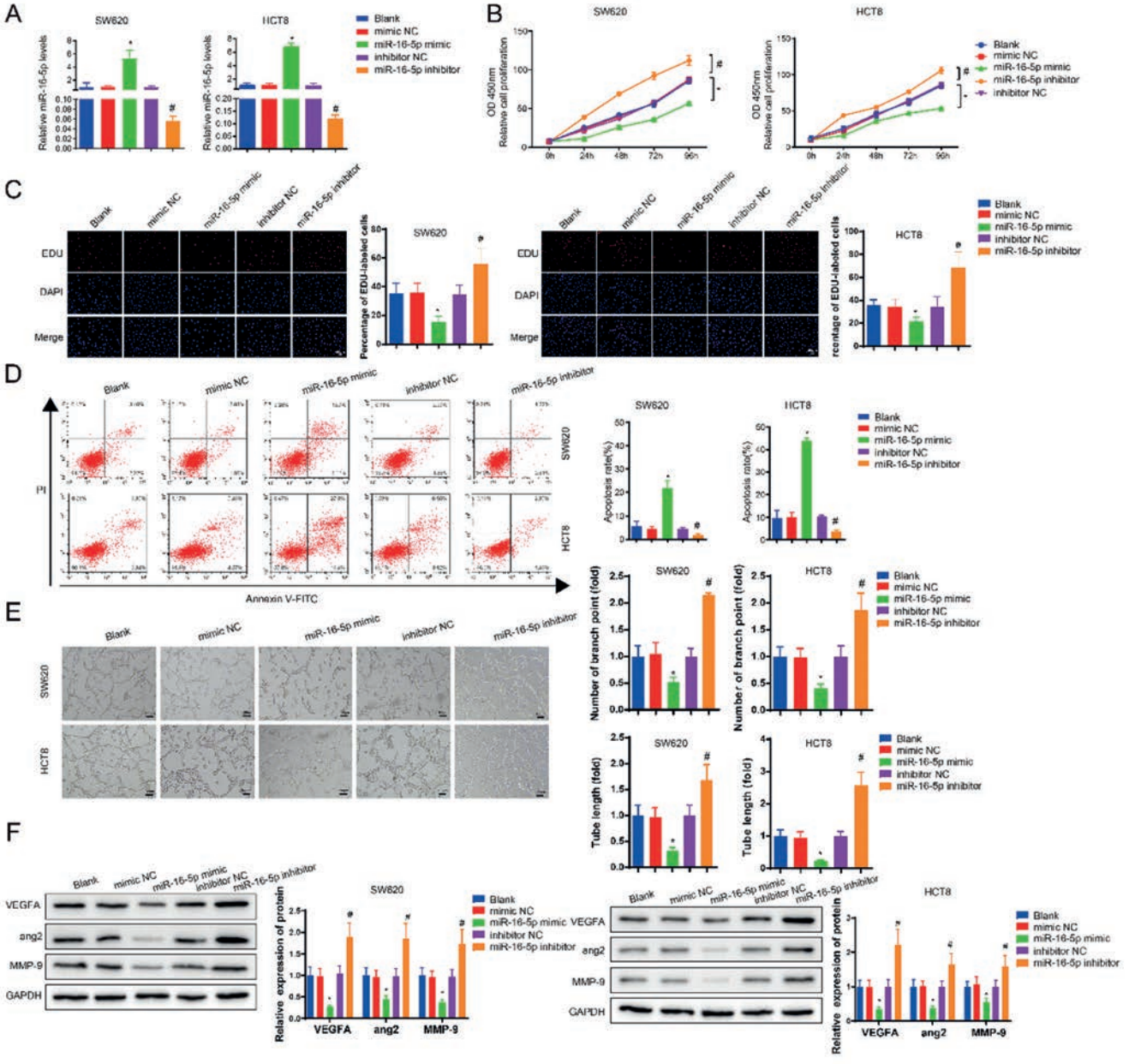

Figure 2. The proliferation, apoptosis, and angiogenesis of CRC cells are related to miR-16-5p. SW620 and HCT8 cells were transfected with miR-16-5p mimic, miR-16-5p inhibitor, and corresponding controls. A) qRT-PCR was utilized for examination of the overexpression/knockdown efficiency of miR-16-5p in SW620 and HCT8 cells. B) CCK-8 assay was applied for analysis of CRC viability. C) EdU assay was adopted for analysis of SW620 and HCT8 cell proliferation ability (×200) (on the left was the representative image of EdU staining, and on the right was a quantitative analysis of the ratio of positive cells). D) Flow cytometry was employed for the detection of CRC cell apoptosis (left side, representative dual-parameter cytograms; right side, percentage of apoptotic cells). E) Tube formation assay was conducted for measurement of HUVEC angiogenesis, evaluated by vessel length and branch points (left side, representative micrographs of tube formation; right side, relative quantitative analysis of tube length and branch points); scale bar: 100 μm. F) Expression of angiogenesis-related proteins (VEGFA, ang2, and MMP-9) was evaluated using Western blot (on the left, representative Western blot bands of VEGFA, ang2, and MMP-9 proteins; on the right, quantitative analysis of the relative protein levels). One-way analysis of variance test was applied for comparison among multiple groups with Tukey's method for *post-hoc* multiple comparisons. Cell experiments were independently repeated three times, and data were expressed as means ±SD. CRC, colorectal cancer; NC, negative control; HUVECs, human umbilical vein endothelial cells; VEGFA, vascular endothelial growth factor A; ang2, Angiopoietin 2; MMP-9, matrix metalloproteinase-9; *$p<0.05$ compared to mimic NC group; #$p<0.05$ compared to inhibitor NC group.

effective transfection of pcDNA3.1-FOXK1 and si-FOXK1 in SW620 and HCT8 cells (Figure 3 A,B; $p<0.05$). Subsequently, CCK-8 and EdU assays depicted a notably declined cell proliferation in the si-FOXK1 group (*vs* the si-NC group) and a prominently augmented proliferation of CRC cells in the pcDNA3.1-FOXK1 group (Figure 3 C,D; *vs* the pcDNA3.1 group, $p<0.05$).

Flow cytometry demonstrated that the knockdown of FOXK1 enhanced CRC cell apoptosis but the overexpression of FOXK1 diminished cell apoptosis (Figure 3E; $p<0.05$). Tube formation assay and Western blot displayed the suppressed tube-forming ability of HUVECs after culture with supernatant of SW620 and HCT8 cells transfected with si-FOXK1, accompanied by diminished VEGFA, ang2, and MMP-9 expression (Figure 3 F,G; *vs* the si-NC group, $p<0.05$) and elevated tube-forming ability and VEGFA, ang2, and MMP-9 expression of HUVECs following culture with supernatant of SW620 and HCT8 cells transfected with pcDNA3.1-FOXK1 (Figure 3 F,G; *v.* the pcDNA3.1 group, $p<0.05$). Collectively, FOXK1 boosted cell proliferation and angiogenesis in CRC.

miR-16-5p negatively regulated FOXK1 in CRC cells

The aforesaid results elucidated that in CRC tissues and cells, miR-16-5p expression was negatively correlated with FOXK1. In an attempt to study whether miR-16-5p mediated FOXK1 in CRC cells, a dual-luciferase reporter assay was utilized for the analysis of the targeting relationship between miR-16-5p and FOXK1. The dual-luciferase reporter assay stated that in the wt-FOXK1 + miR-16-5p mimic group, the luciferase activity was diminished with the enhancement in miR-16-5p mimic concentration compared with the wt-FOXK1 + mimic-NC group (Figure 4A, $p<0.05$), and no obvious difference in luciferase activity was revealed between the mut-FOXK1 + miR-16-5p mimic group and the mut-FOXK1 + mimic-NC group (Figure 4A, $p>0.05$). These results indicated that miR-16-5p targeted FOXK1.

Subsequently, the analyses of qRT-PCR and Western blot further ascertained the targeting relationship between miR-16-5p and FOXK1. miR-16-5p mimic reduced the mRNA and protein levels of FOXK1 in SW620 and HCT8 cells, whereas miR-16-5p inhibitor elevated FOXK1 expression (Figure 4 B,C, $p<0.05$). These data revealed that miR-16-5p negatively targeted FOXK1 in CRC cells.

miR-16-5p blocked the PI3K/Akt/mTOR pathway by downregulating FOXK1

To further delve into whether miR-16-5p modulated cell angiogenesis, apoptosis, and proliferation in CRC by targeting FOXK1, SW620 and HCT8 cells were co-transfected with miR-16-5p mimic and pcDNA3.1-FOXK1. As reflected by the results of CCK-8 assay (Figure 5A), EdU assay (Figure 5B), and flow cytometry (Figure 5C), transfection with miR-16-5p mimic augmented the apoptotic rate and diminished cell proliferation of SW620 and HCT8 cells, whereas pcDNA3.1-FOXK1 transfection caused contrary results ($p<0.05$). Tube formation assay (Figure 5D) and Western blot (Figure 5E) manifested that the tube-forming ability and VEGFA, ang2, and MMP-9 expression of HUVECs were diminished by co-culture with the supernatant of miR-16-5p mimic-transfected SW620 and HCT8 cells but enhanced by co-culture with the supernatant of pcDNA3.1-FOXK1-transfected SW620 and HCT8 cells ($p<0.05$). Co-transfection of miR-16-5p mimic and pcDNA3.1-FOXK1 counteracted the suppressive effect of miR-16-5p mimic on the above indicators (Figure 5A-E; $p<0.05$). In conclusion, miR-16-5p induced cell apoptosis and curtailed cell proliferation and angiogenesis by targeting FOXK1 in CRC.

Western blot was employed to assess the relationship between miR-16-5p and the PI3K/Akt/mTOR pathway. Transfection with the miR-16-5p mimic decreased the phosphorylation of PI3K, Akt, and mTOR in SW620 and HCT8 cells, and transfection with pcDNA3.1-FOXK1 enhanced the phosphorylation of PI3K, Akt, and mTOR in SW620 and HCT8 cells. However, the difference in these phosphorylation levels did not reach statistical significance among the blank, mimic-NC, and pcDNA3.1 groups. Furthermore, co-transfection with miR-16-5p mimic and pcDNA3.1-FOXK1 increased the phosphorylation of pathway-related proteins (Figure 5F-G; $p<0.05$, *vs* the miR-16-5p mimic group). Taken together, miR-16-5p disrupted the PI3K/Akt/mTOR pathway by repressing FOXK1.

Discussion

As one of the most prevalent malignancies currently, CRC confers a high fatality and incidence rate worldwide despite advances in diagnosis and therapy.[23,24] It is indispensable for future therapeutic strategies of CRC to detect innovative screening biomarkers and study their mechanisms that manipulate CRC progression.[25] It is therefore imperative to address the molecular mechanism underlying CRC pathology to develop therapeutic strategies for CRC. In this study, colon cancer cell lines SW620 and HCT8 were utilized to analyze the impacts of miR-16-5p and FOXK1 on the proliferation and apoptosis of CRC cells and the angiogenesis of HUVECs co-incubated with the supernatant of CRC cells. Moreover, we found that miR-16-5p negatively targeted FOXK1 to block the PI3K/Akt/mTOR pathway, which subdued cell proliferation and angiogenesis in CRC.

miR-16-5p and FOXK1 expression was examined by qRT-PCR and the results exhibited that miR-16-5p was lowly expressed and FOXK1 was highly expressed in CRC tissues and cells. Interestingly, prior studies have analyzed that CRC tissues contain elevated FOXK1 expression and downregulated miR-16-5p expression compared with normal colonic tissues.[26-28] From these preliminary observations, we gave an assumption that miR-16-5p may inhibit tumorigenesis in CRC. CCK-8 assay, EdU assay, and flow cytometry further confirmed our hypothesis that miR-16-5p promoted apoptosis and repressed proliferation of CRC cells. Such changes were consistent with angiogenesis observed in HUVECs by tube-forming assay. Our results are in agreement with the findings by Wu *et al*., manifesting that miR-16-5p can hinder cell proliferation, invasion, migration, and angiogenesis in CRC.[14] Also, Xu *et al*.[29] noted that ectopically expressed miR-16-5p stimulated apoptosis while repressing the proliferative, migratory, and invasive capacity of CRC cells. Although miR-16-5p is well explored for its anti-oncogenic effects, miR-16-5p has been also reported to orchestrate multiple physiological or immunological processes. For instance, miR-16-5p acts as a positive feedback mediator in EV71-induced apoptosis and an inhibitor of virus replication.[30] miR-16-5p downregulation restricted endoplasmic reticulum of human cardiomyocytes and oxidative stress-induced injury.[31] In addition, miR-16-5p has been documented to predict poor immune response following antiretroviral therapy in HIV-infected patients.[32] Also, Li *et al*. observed that miR-16-5p was involved in the promoting effects of M1 macrophage-released exosomes on T cell-dependent immune response *via* PD-L1 in GC. Therefore, future investigations are warranted to further ascertain the role of miR-16-5p in physiological or immunological processes.

Furthermore, we found highly expressed FOXK1 fostered angiogenesis and proliferation in CRC cells. FOXK1, which is associated with multiple malignancies, confers an essential effect on cell proliferation, metastasis, apoptosis, and cell cycle transition.[33,34] For instance, FOXK1 is reported to promote cell prolifer-

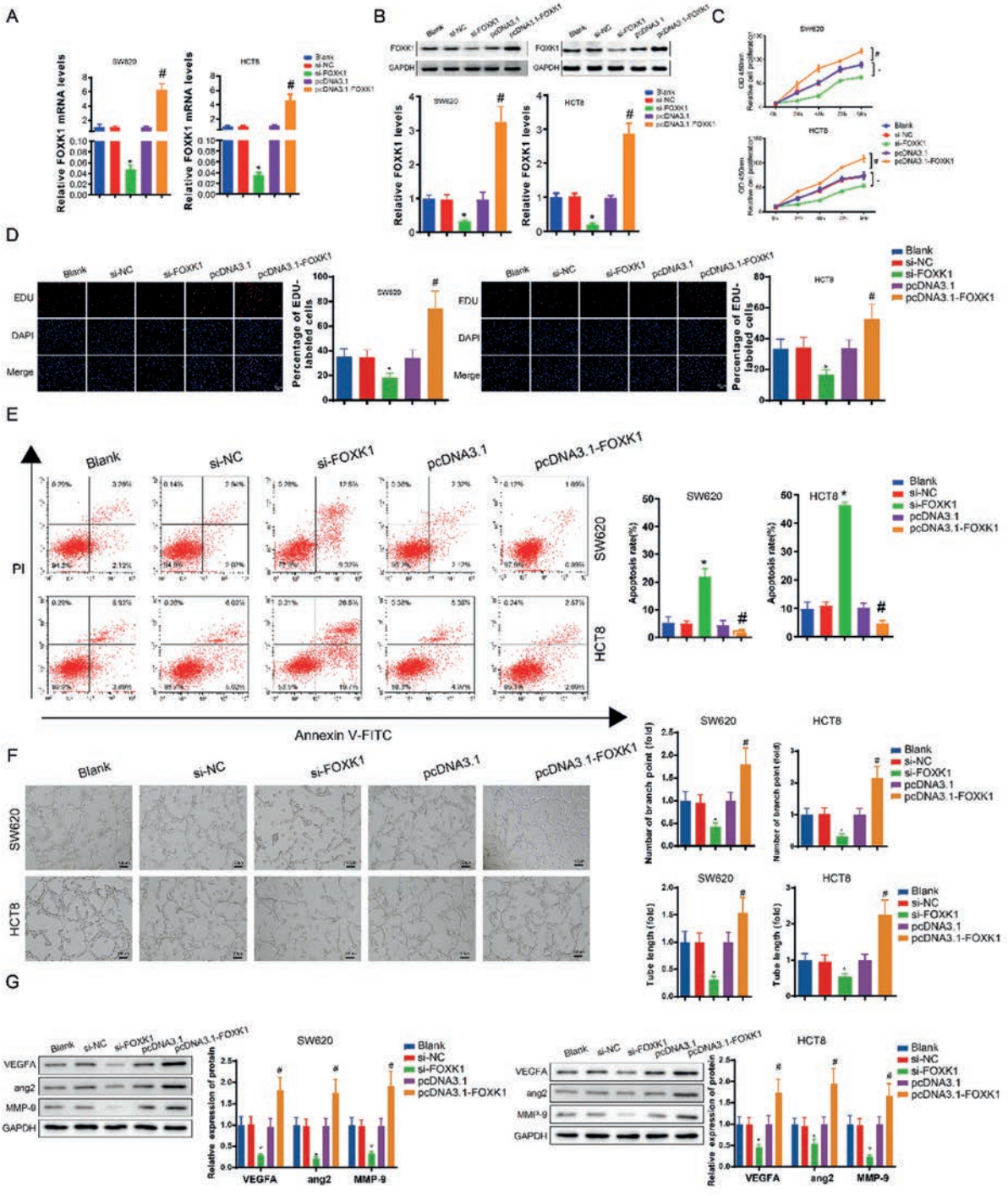

Figure 3. FOXK1 plays a vital role in CRC cell proliferation, apoptosis, and angiogenesis. SW620 and HCT8 cells were transfected with si-FOXK1 and pcDNA3.1-FOXK1 and their corresponding NCs. A) The overexpression/knockdown efficiency of FOXK1 in SW620 and HCT8 cells was detected by qRT-PCR. B) The overexpression/knockdown efficiency of FOXK1 in SW620 and HCT8 cells was evaluated by Western blot (upper row, representative Western blot of FOXK1 protein; lower row, quantitative analysis of the relative FOXK1protein levels). C) SW620 and HCT8 cell viability was tested by CCK-8 assay. D) SW620 and HCT8 cell proliferation ability was assessed by EdU assay (×200) (on the left, representative images of EdU staining; on the right, percentage of positive cells). E) SW620 and HCT8 cell apoptosis was evaluated by flow cytometry (left side, representative flow cytograms; right side, quantitative analysis of the apoptosis rate). F) The tube formation assay was conducted for measurement of HUVEC angiogenesis, evaluated by vessel length and branch points (scale bar: 100 μm) (left side, representative micrographs of tube formation; right side, quantitative analysis of the tube length and branch points). G) Expression of VEGFA, ang2, and MMP-9 was evaluated by Western blot (left side, representative Western blot of VEGFA, ang2, and MMP-9 proteins; right side, quantitative analysis of relative protein levels). One-way analysis of variance test was applied for comparison among multiple groups with Tukey's method for post hoc multiple comparisons. Cell experiments were independently repeated three times, and data were expressed as means ±SD. CRC, colorectal cancer; NC, negative control; HUVECs, human umbilical vein endothelial cells; VEGFA, vascular endothelial growth factor A; ang2, Angiopoietin 2; MMP-9, matrix metalloproteinase-9; *p<0.05 compared to the si-NC group; #p<0.05 compared to the pcDNA3.1 group.

ation *via* p21 and facilitate metastasis in ovarian cancer.[35] Moreover, FOXK1 can induce epithelial-to-mesenchymal transition and promote proliferation, invasion, and metastasis in CRC cells.[36,37] Correspondingly, our findings revealed that the transfection of miR-16-5p mimic hampered the mRNA and protein expression of FOXK1, whereas the transfection of miR-16-5p inhibitor augmented FOXK1 expression. FOXK1 and miR-16-5p have been studied in association with CRC, and qRT-PCR revealed a negative correlation between FOXK1 and miR-16-5p expression. Thus, we hypothesized that FOXK1 was a target gene of miR-16-5p, which was confirmed by the dual-luciferase reporter assay. Taken together, these results provided a possible ideal that the miR-16-5p/FOXK1 axis could control cell proliferation and angiogenesis in CRC. Since the effect of FOXK1 on cell proliferation and angiogenesis in CRC was orchestrated by miR-16-5p, the most likely explanation was that miR-16-5p targeted FOXK1 to inhibit angiogenesis and proliferation in CRC. Subsequently, this finding was confirmed by rescue experiments.

The PI3K/Akt/mTOR pathway, an intracellular pathway, is directly associated with cell proliferation, longevity, and cancer.[38] In this study, we identified that miR-16-5p was an inhibitor of the PI3K/Akt/mTOR pathway in CRC cells, which is similar to the previous finding.[39] mTOR, the downstream factor of the PI3K/Akt pathway, is a possible therapy for various types of cancer, including CRC.[40] The activated PI3K phosphorylates 3, 4, 5-phosphatidylinositol trisphosphate, which thereafter activates Akt and mTOR and affects cell proliferation, growth, and other functions.[40,41] Our results exhibited that the overexpression of FOXK1 accelerated the activation of the PI3K/Akt/mTOR pathway, whereas the overexpression of miR-16-5p led to the opposite result. Furthermore, the PI3K/Akt/mTOR pathway was involved in the angiogenesis and proliferation of CRC, which was negatively mediated by miR-16-5p. To conclude, the abnormal expression pattern of miR-16-5p and FOXK1 was associated with the progres-

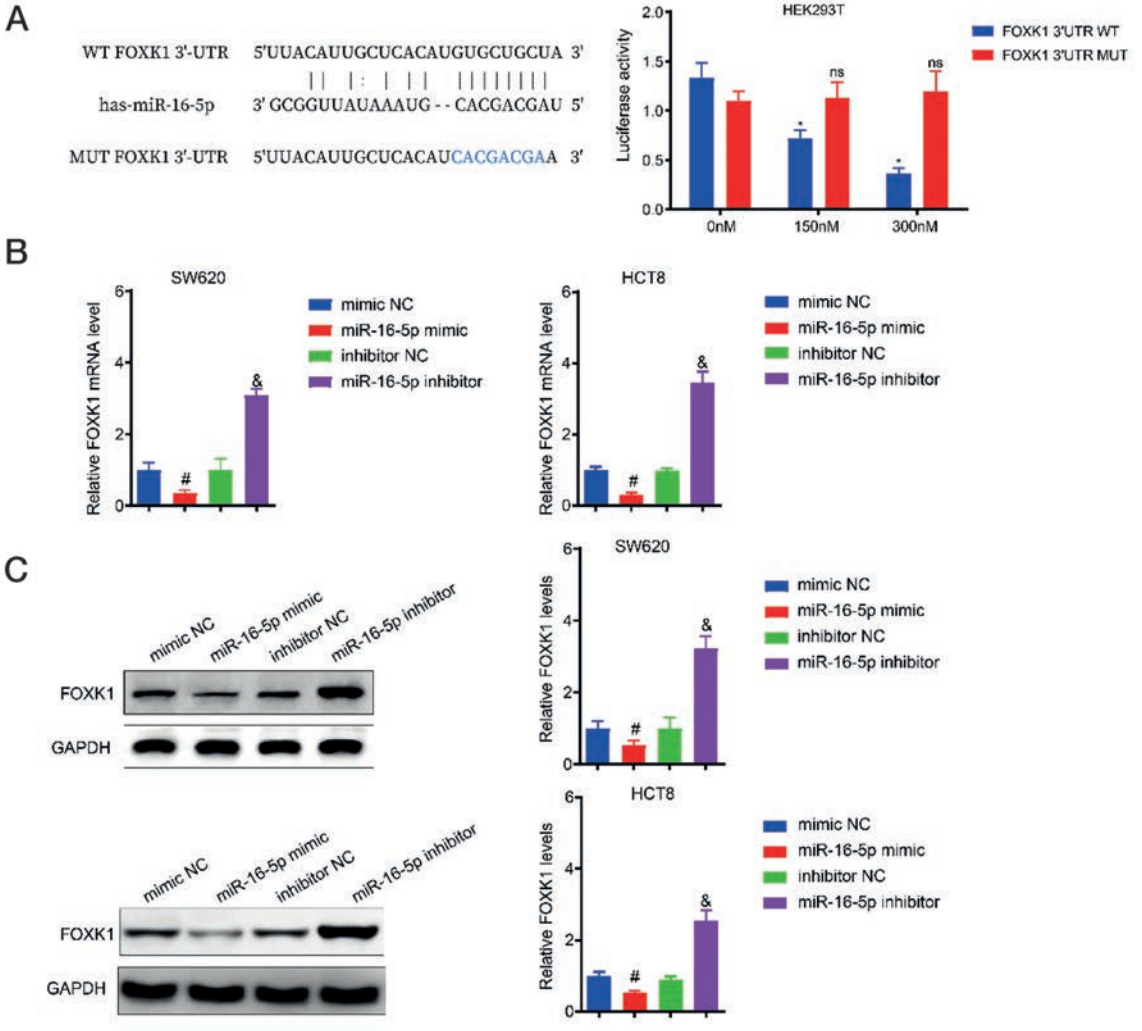

Figure 4. FOXK1 is inversely targeted by miR-16-5p in CRC cells. A) The binding site of FOXK1 to miR-16-5p was predicted based on the StarBase database with mutation site of FOXK1 designed and synthesized (left) and a dual-luciferase reporter gene assay was conducted to verify the binding relationship between miR-16-5p and FOXK1 (right). B) qRT-PCR was applied to detect the effect of miR-16-5p on FOXK1 mRNA expression. C) Western blot was adopted to test the effect of miR-16-5p on FOXK1 protein expression (left side, representative Western blot of FOXK1; right side, quantitative analysis of FOXK1 relative protein level). One-way analysis of variance test was applied for comparison among multiple groups with Tukey's method for *post-hoc* multiple comparisons. Cell experiments were independently repeated three times, and data were expressed as means ±SD. CRC, colorectal cancer; NC, negative control; *p<0.05 compared to the wt-FOXK1 group; ns p>0.05; #p<0.05 compared to the mimic-NC group; &p<0.05 compared to the inhibitor NC group.

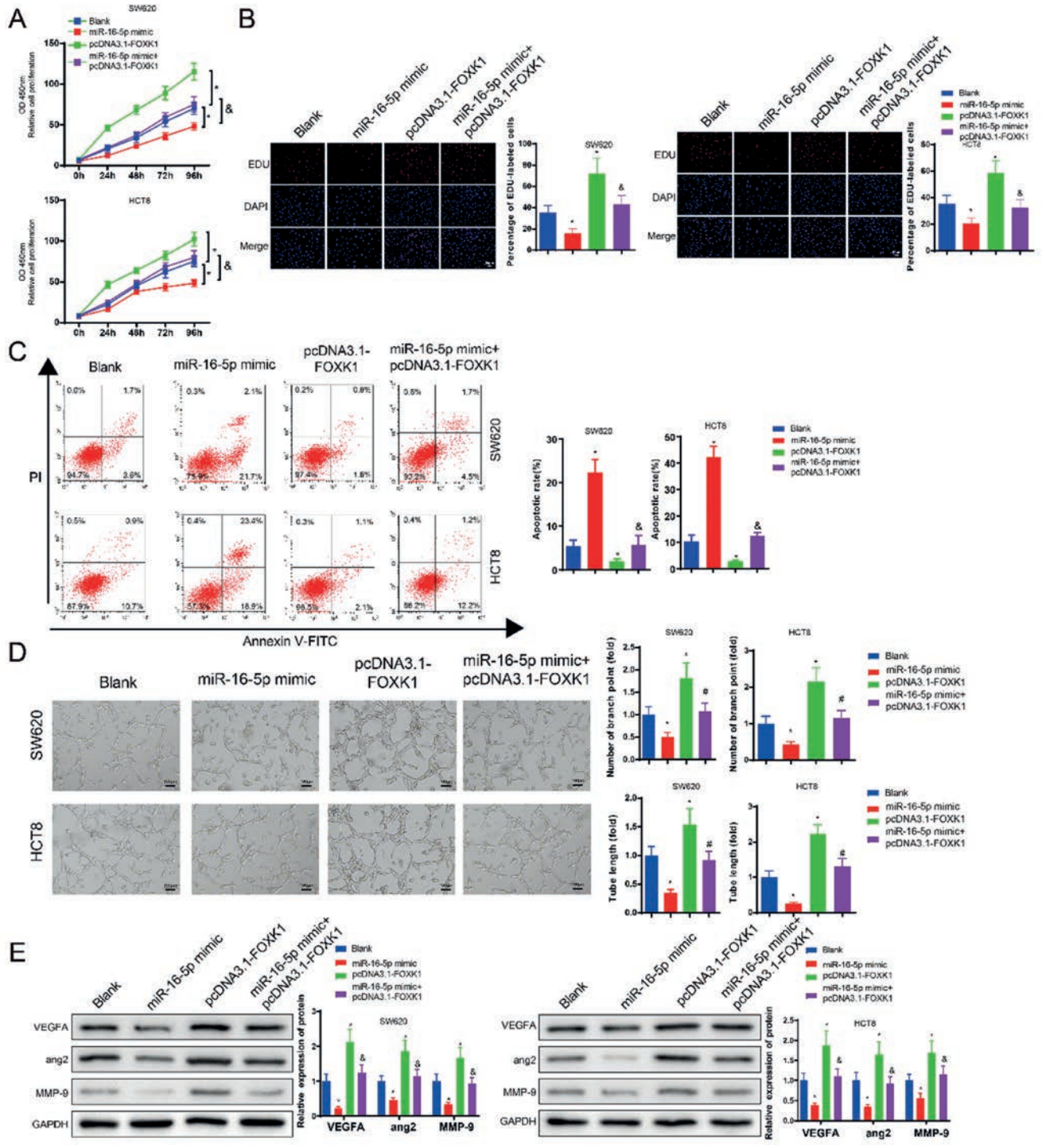

Figure 5 A-E. **The PI3K/Akt/mTOR pathway is curbed by miR-16-5p by targeting FOXK1 in CRC cells. SW620 and HCT8 cells were transfected or co-transfected with miR-16-5p mimic and pcDNA3.1-FOXK1. A) CCK-8 assay was used to measure the viability of SW620 and HCT8 cells. B) EdU assay was performed to assess the proliferation ability of SW620 and HCT8 cells (× 200) (on the left, representative images of EdU staining; on the right, percentage of positive cells). C) Flow cytometry was applied to detect cell apoptotic rate (left side, representative cytograms; right side, apoptosis rate). D) Tube formation assay was employed to assess the tube-forming ability of HUVECs, evaluated by tube length and branch points (scale bar: 100 μm) (left side, representative micrographs of tube formation; right side, relative quantitative analysis of the tube length and branch points). E) Expression of VEGFA, ang2, and MMP-9 was evaluated by Western blot (left side, representative Western blot bands of VEGFA, ang2, and MMP-9 proteins; right side, relative protein levels). CRC, colorectal cancer; NC, negative control; HUVECs, human umbilical vein endothelial cells; VEGFA, vascular endothelial growth factor A; ang2, Angiopoietin 2; MMP-9, matrix metalloproteinase-9; PI3K, phosphoinositide 3-kinase; mTOR, mechanistic target of rapamycin; *p<0.05 compared to the blank group; $^{\#}$p<0.05 compared to the mimic-NC group; $^{\$}$p<0.05 compared to the pcDNA3.1 group; $^{\&}$p<0.05 compared to the miR-16-5p mimic group.**

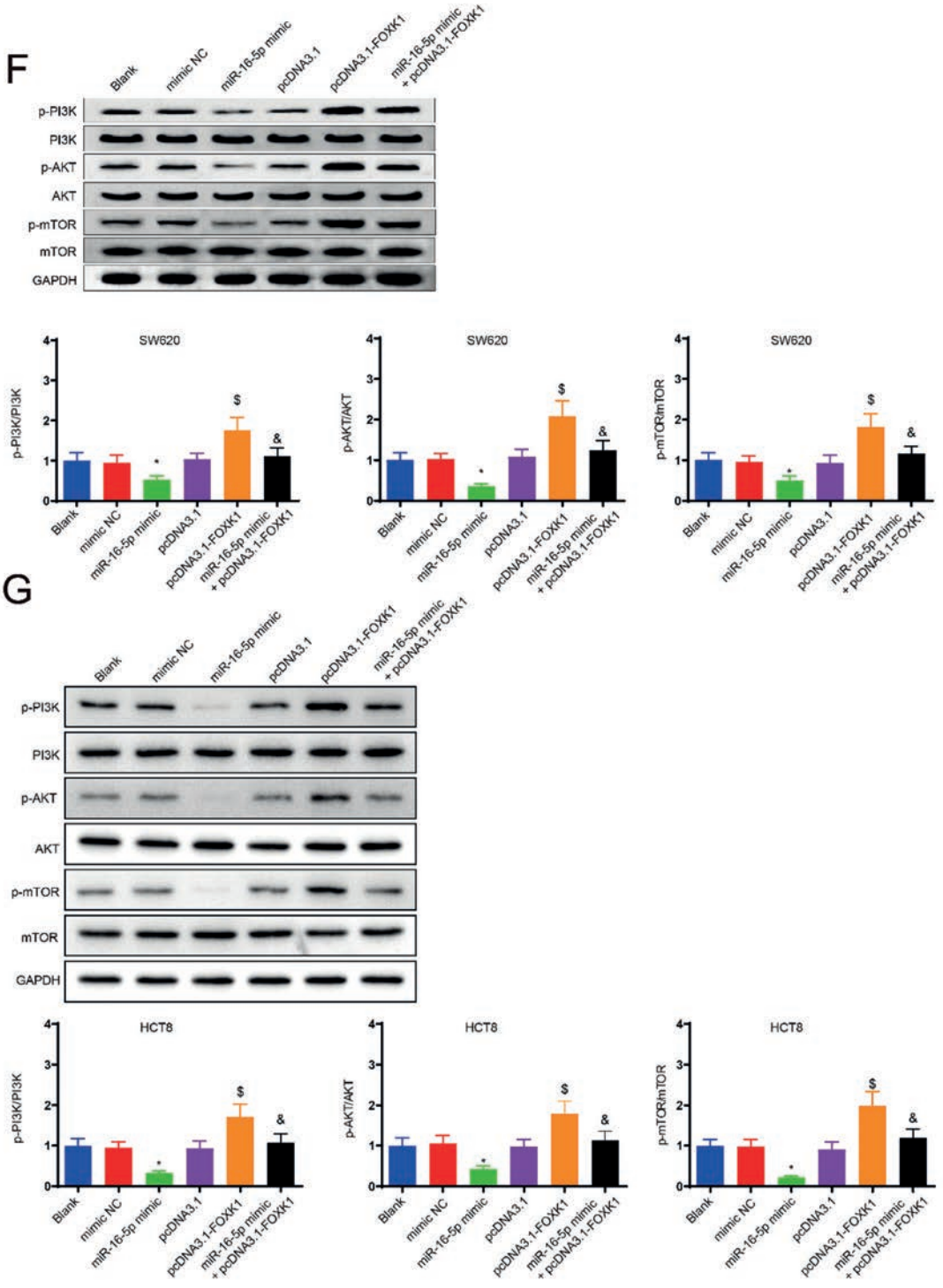

Figure 5 F-G. The PI3K/Akt/mTOR pathway is curbed by miR-16-5p by targeting FOXK1 in CRC cells. SW620 and HCT8 cells were transfected or co-transfected with miR-16-5p mimic and pcDNA3.1-FOXK1. F) The expression and phosphorylation levels of PI3K, Akt, and mTOR in SW620 cells were measured by Western blot (upper side row, representative Western blot bands of p-PI3K, p-Akt, p-mTOR, PI3K, Akt, and mTOR; lower row, relative protein and phosphorylation levels). G) The expression and phosphorylation levels of PI3K, Akt, and mTOR in HCT8 cells were evaluated by Western blot (upper row, representative Western blot bands of p-PI3K, p-Akt, p-mTOR, PI3K, Akt, and mTOR; and the lower side was the quantitative analysis of relative protein and phosphorylation levels). One-way analysis of variance test was applied for comparison among multiple groups with Tukey's method for post hoc multiple comparisons. Cell experiments were independently repeated three times, and data were expressed as means ±SD. CRC, colorectal cancer; NC, negative control; HUVECs, human umbilical vein endothelial cells; VEGFA, vascular endothelial growth factor A; ang2, Angiopoietin 2; MMP-9, matrix metalloproteinase-9; PI3K, phosphoinositide 3-kinase; mTOR, mechanistic target of rapamycin; *p<0.05 compared to the blank group; #p<0.05 compared to the mimic-NC group; $p<0.05 compared to the pcDNA3.1 group; &p<0.05 compared to the miR-16-5p mimic group.

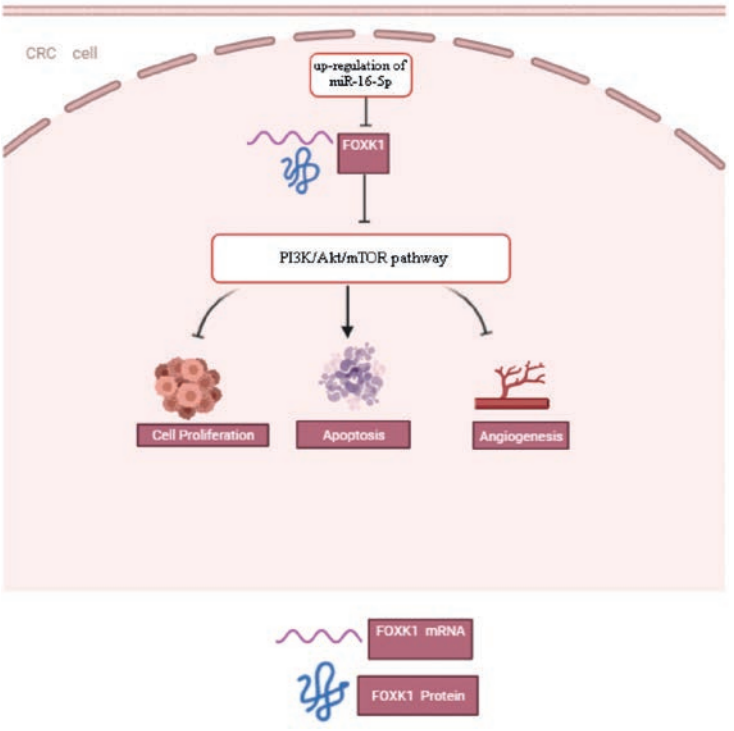

Figure 6. Schematic diagram. miR-16-5p suppresses cell proliferation and angiogenesis in colorectal cancer by blocking the PI3K/Akt/mTOR pathway through FOXK1.

sion of CRC, and FOXK1 possessed the ability to promote cell proliferation and angiogenesis in CRC (Figure 6). miR-16-5p exerted a potent tumor-suppressing role in CRC through the blockade of the PI3K/Akt/mTOR pathway by negatively regulating FOXK1. Thus, this study provided novel evidence that miR-16-5p targeting FOXK1 may be a novel and promising therapeutic approach to the treatment of CRC. However, there are some limitations to this study. Firstly, the effects of miR-16-5p and FOXK1 on migration and invasion of CRC cells were not explored, and no *in vivo* experiments were performed for the time being. We will further explore the effects of miR-16-5p and FOXK1 on migration and invasion of CRC cells and the regulatory role of miR-16-5p and FOXK1 on tumors in animal models of transplantation tumor *in vivo* in the future. Secondly, based on tissue results and *in vitro* results published in this report, further investigations are warranted to identify the role of miR-16-5p in patient samples in order to find the correlation of miR-16-5p with tumorigenesis, metastasis, and prognosis and reveal the therapeutic potential of miR-16-5p in CRC.

Acknowledgements

We thank the Jiangxi Clinical Research Center for Gastroenterology (No. 20201ZDG02007) for their contribution to the study.

References

1. Lan J, Li H, Luo X, Hu J, Wang G. BRG1 promotes VEGF-A expression and angiogenesis in human colorectal cancer cells. Exp Cell Res 2017;360:236-42.
2. Wei R, Yang Q, Han B, Li Y, Yao K, Yang X, et al. microRNA-375 inhibits colorectal cancer cells proliferation by downregulating JAK2/STAT3 and MAP3K8/ERK signaling pathways. Oncotarget 2017;8:16633-41.
3. Jeon J, Du M, Schoen RE, Hoffmeister M, Newcomb PA, Berndt SI, et al. Determining risk of colorectal cancer and starting age of screening based on lifestyle, environmental, and genetic factors. Gastroenterology 2018;154:2152-64.e19.
4. Zhu P, Wu Y, Yang A, Fu X, Mao M, Liu Z. Catalpol suppressed proliferation, growth and invasion of CT26 colon cancer by inhibiting inflammation and tumor angiogenesis. Biomed Pharmacother 2017;95:68-76.
5. Sun D, Zhang F, Qian J, Shen W, Fan H, Tan J, et al. 4'-hydroxywogonin inhibits colorectal cancer angiogenesis by disrupting PI3K/AKT signaling. Chem Biol Interact 2018;296:26-33.
6. Tawfik MK, Mohamed MI. Exenatide suppresses 1,2-dimethylhydrazine-induced colon cancer in diabetic mice: Effect on tumor angiogenesis and cell proliferation. Biomed Pharmacother 2016;82:106-16.
7. Yang Y, Bao Y, Yang GK, Wan J, Du LJ, Ma ZH. MiR-214 sensitizes human colon cancer cells to 5-FU by targeting Hsp27. Cell Mol Biol Lett 2019;24:22.
8. Ding L, Yu LL, Han N, Zhang BT. miR-141 promotes colon cancer cell proliferation by inhibiting MAP2K4. Oncol Lett 2017;13:1665-71.
9. Vychytilova-Faltejskova P, Radova L, Sachlova M, Kosarova Z, Slaba K, Fabian P, et al. Serum-based microRNA signatures in early diagnosis and prognosis prediction of colon cancer. Carcinogenesis 2016;37:941-50.
10. Zeng M, Zhu L, Li L, Kang C. miR-378 suppresses the proliferation, migration and invasion of colon cancer cells by inhibiting SDAD1. Cell Mol Biol Lett 2017;22:12.
11. Basu A, Jiang X, Negrini M, Haldar S. MicroRNA-mediated regulation of pancreatic cancer cell proliferation. Oncol Lett 2010;1:565-8.

12. Jia X, Li X, Shen Y, Miao J, Liu H, Li G, et al. MiR-16 regulates mouse peritoneal macrophage polarization and affects T-cell activation. J Cell Mol Med 2016;20:1898-907.
13. Li N, Yang L, Sun Y, Wu X. MicroRNA-16 inhibits migration and invasion via regulation of the Wnt/beta-catenin signaling pathway in ovarian cancer. Oncol Lett 2019;17:2631-8.
14. Wu H, Wei M, Jiang X, Tan J, Xu W, Fan X, et al. lncRNA PVT1 promotes tumorigenesis of colorectal cancer by stabilizing miR-16-5p and interacting with the VEGFA/VEGFR1/AKT axis. Mol Ther Nucleic Acids 2020;20:438-50.
15. Zhu T, Lin Z, Han S, Wei Y, Lu G, Zhang Y, et al. Low miR-16 expression induces regulatory CD4(+)NKG2D(+) T cells involved in colorectal cancer progression. Am J Cancer Res 2021;11:1540-56.
16. Huang X, Hou Y, Weng X, Pang W, Hou L, Liang Y, et al. Diethyldithiocarbamate-copper complex (CuET) inhibits colorectal cancer progression via miR-16-5p and 15b-5p/ALDH1A3/PKM2 axis-mediated aerobic glycolysis pathway. Oncogenesis 2021;10:4.
17. Gao F, Tian J. FOXK1, regulated by miR-365-3p, promotes cell growth and EMT indicates unfavorable prognosis in breast cancer. Onco Targets Ther 2020;13:623-34.
18. Garry DJ, Maeng G, Garry MG. Foxk1 regulates cancer progression. Ann Transl Med 2020;8:1041.
19. Wang Y, Qiu W, Liu N, Sun L, Liu Z, Wang S, et al. Forkhead box K1 regulates the malignant behavior of gastric cancer by inhibiting autophagy. Ann Transl Med 2020;8:107.
20. Feng Y, Bai Z, Song J, Zhang Z. FOXK1 plays an oncogenic role in the progression of hilar cholangiocarcinoma. Mol Med Rep 2021;23:91.
21. Wang J, Liu G, Liu M, Xiang L, Xiao Y, Zhu H, et al. The FOXK1-CCDC43 axis promotes the invasion and metastasis of colorectal cancer cells. Cell Physiol Biochem 2018;51:2547-63.
22. Xie R, Wang J, Liu X, Wu L, Zhang H, Tang W, et al. RUFY3 interaction with FOXK1 promotes invasion and metastasis in colorectal cancer. Sci Rep 2017;7:3709.
23. Li C, Xu N, Li YQ, Wang Y, Zhu ZT. Inhibition of SW620 human colon cancer cells by upregulating miRNA-145. World J Gastroenterol 2016;22:2771-8.
24. Zheng B, Chen L, Pan CC, Wang JZ, Lu GR, Yang SX, et al. Targeted delivery of miRNA-204-5p by PEGylated polymer nanoparticles for colon cancer therapy. Nanomedicine (Lond) 2018;13:769-85.
25. Fang X, Hong Y, Dai L, Qian Y, Zhu C, Wu B, et al. CRH promotes human colon cancer cell proliferation via IL-6/JAK2/STAT3 signaling pathway and VEGF-induced tumor angiogenesis. Mol Carcinog 2017;56:2434-45.
26. Liu Y, Zhou J, Wang S, Song Y, Zhou J, Ren F. Long non-coding RNA SNHG12 promotes proliferation and invasion of colorectal cancer cells by acting as a molecular sponge of microRNA-16. Exp Ther Med 2019;18:1212-20.
27. Cheng B, Ding F, Huang CY, Xiao H, Fei FY, Li J. Role of miR-16-5p in the proliferation and metastasis of hepatocellular carcinoma. Eur Rev Med Pharmacol Sci 2019;23:137-45.
28. Wu W, Chen Y, Ye S, Yang H, Yang J, Quan J. Transcription factor forkhead box K1 regulates miR-32 expression and enhances cell proliferation in colorectal cancer. Oncol Lett 2021;21:407.
29. Xu Y, Shen L, Li F, Yang J, Wan X, Ouyang M. microRNA-16-5p-containing exosomes derived from bone marrow-derived mesenchymal stem cells inhibit proliferation, migration, and invasion, while promoting apoptosis of colorectal cancer cells by downregulating ITGA2. J Cell Physiol 2019;234:21380-94.
30. Zheng C, Zheng Z, Sun J, Zhang Y, Wei C, Ke X, et al. MiR-16-5p mediates a positive feedback loop in EV71-induced apoptosis and suppresses virus replication. Sci Rep 2017;7:16422.
31. Toro R, Perez-Serra A, Mangas A, Campuzano O, Sarquella-Brugada G, Quezada-Feijoo M, et al. miR-16-5p suppression protects human cardiomyocytes against endoplasmic reticulum and oxidative stress-induced injury. Int J Mol Sci 2022;23:1036.
32. Lv JN, Li JQ, Cui YB, Ren YY, Fu YJ, Jiang YJ, et al. Plasma microRNA signature panel predicts the immune response after antiretroviral therapy in HIV-infected patients. Front Immunol 2021;12:753044.
33. Ji ZG, Jiang HT, Zhang PS. FOXK1 promotes cell growth through activating wnt/beta-catenin pathway and emerges as a novel target of miR-137 in glioma. Am J Transl Res 2018;10:1784-92.
34. Xu H, Huang S, Zhu X, Zhang W, Zhang X. FOXK1 promotes glioblastoma proliferation and metastasis through activation of Snail transcription. Exp Ther Med 2018;15:3108-16.
35. Li L, Gong M, Zhao Y, Zhao X, Li Q. FOXK1 facilitates cell proliferation through regulating the expression of p21, and promotes metastasis in ovarian cancer. Oncotarget 2017;8:70441-51.
36. Wu M, Wang J, Tang W, Zhan X, Li Y, Peng Y, et al. FOXK1 interaction with FHL2 promotes proliferation, invasion and metastasis in colorectal cancer. Oncogenesis 2016;5:e271.
37. Wu Y, Peng Y, Wu M, Zhang W, Zhang M, Xie R, et al. Oncogene FOXK1 enhances invasion of colorectal carcinoma by inducing epithelial-mesenchymal transition. Oncotarget 2016;7:51150-62.
38. Zhang D, Wang S, Chen J, Liu H, Lu J, Jiang H, et al. Fibulin-4 promotes osteosarcoma invasion and metastasis by inducing epithelial to mesenchymal transition via the PI3K/Akt/mTOR pathway. Int J Oncol 2017;50:1513-30.
39. Ghafouri-Fard S, Abak A, Tondro Anamag F, Shoorei H, Majidpoor J, Taheri M. The emerging role of non-coding RNAs in the regulation of PI3K/AKT pathway in the carcinogenesis process. Biomed Pharmacother 2021;137:111279.
40. Zhang X, Shi H, Tang H, Fang Z, Wang J, Cui S. miR-218 inhibits the invasion and migration of colon cancer cells by targeting the PI3K/Akt/mTOR signaling pathway. Int J Mol Med 2015;35:1301-8.
41. Liu Y, Bi T, Wang Z, Wu G, Qian L, Gao Q, et al. Oxymatrine synergistically enhances antitumor activity of oxaliplatin in colon carcinoma through PI3K/AKT/mTOR pathway. Apoptosis 2016;21:1398-407.

Received for publication: 13 September 2021. Accepted for publication: 23 March 2022.

Licensee PAGEPress, Italy
European Journal of Histochemistry 2022; 66:3333
doi:10.4081/ejh.2022.3333